FLUID INCLUSIONS IN PORPHYRY-TYPE DEPOSITS

R. J. Bodnar

Bodnar

Mineral Deposits Research Review for Industry

Tuesday Night, April 6

7:00 to 9:00	Registration and reception at The Nittany Lion Inn (Complimentary bar and hors d'oeuvres)	

Wednesday, April 7

8:30 to 9:00	Welcome	C. W. Burnham D. Noyes H. L. Barnes L. M. Cathles

Morning—Magmatic Systems and Fluid Inclusions
Moderator: D. P. (Duff) Gold

9:00 to 9:45	Magmatic Fluids	C. W. Burnham
9:45 to 10:05	Discussion	
10:05 to 10:25	Coffee	
10:25 to 11:10	Fluid Inclusions in Porphyry-type Deposits	R. J. Bodnar
11:10 to 11:30	Discussion	
11:30 to 12:00	Detailed Geologic History from Very Limited Samples: A Case Study	J. B. Murowchick
12:00 to 12:15	Discussion	
12:15 to 1:30	Lunch—The Nittany Lion Inn	

Afternoon—Skarns, Massive Sulfide Deposits, Diamonds, Heavy Minerals
Moderator: A. W. (Art) Rose

1:30 to 2:00	W-Mo Mineralization at King Island, Tasmania	D. Wesolowski
2:00 to 2:30	Mineral Textures and the Formation of Kuroko-type Volcanogenic Massive Sulfide Deposits	C. S. Eldridge
2:30 to 2:50	Discussion	
2:50 to 3:10	Coffee	
3:10 to 3:55	Field Exploration for Diamonds--Where to find, how to locate pipes	D. P. Gold
3:55 to 4:15	Discussion	
4:15 to 5:00	Heavy Mineral Concentrations in Streams: Origin and Prediction	R. Slingerland
5:00 to 5:20	Discussion	
6:30	Social (Cash Bar)	
7:30	Dinner—Elk's Country Club	

Thursday, April 8 GOLD MINERALIZATION

Morning—Gold Geochemistry
Moderator: L. M. (Larry) Cathles

8:30 to 9:30	Geochemistry of Gold Deposits	H. Ohmoto
9:30 to 9:45	Discussion	
9:45 to 10:05	Coffee	
10:05 to 10:35	Alteration Around Gold Deposits	A. W. Rose
10:35 to 10:50	Discussion	
10:50 to 11:20	Gold in Geothermal Systems--Solubility, Transport and Deposition Processes	H. L. Barnes
11:20 to 12:00	Discussion	
12:00 to 1:30	Lunch—The Nittany Lion Inn	

Afternoon—Metamorphic Gold, Hydrodynamics, Fluid Inclusions
Moderator: H. (Hiroshi) Ohmoto

1:30 to 2:00	A Genetic Model for Gold Deposition in Metabasic Rocks	D. M. Kerrick
2:00 to 2:15	Discussion	
2:15 to 2:45	Hydrologic Aspects of Gold Deposits	L. M. Cathles
2:45 to 3:00	Discussion	
3:00 to 3:20	Coffee	
3:20 to 4:20	What Fluid Inclusions Can Tell Us About Au Mineralization: The System H_2O-CO_2-NaCl	C. A. Kuehn R. J. Bodnar
4:20 to 5:30	Discussion	
6:00	Social—Toftrees Country Club	
7:00	Dinner—Toftrees Country Club Speaker: Dr. John E. Tilton Professor of Mineral Economics Topic: "The Continuing Debate over Resource Exhaustion"	

Friday, April 9

Morning—Exploration Geochemistry
Moderator: H. L. (Hu) Barnes

8:30 to 9:15	Mode of Occurrence of Metals in Soils and Stream Sediments and Methods of Chemical Extraction	A. W. Rose
9:15 to 9:35	Discussion	
9:35 to 10:05	SOLUPLOT Calculations and Natural Waters	C. M. Bethke
10:05 to 10:20	Discussion	

Friday Morning Continued

10:20 to 10:50	Geologic and Geochemical Controls on Cu-U Mineralization in Red Beds--Catskill Formation	A. T. Smith
10:50 to 11:20	The Organic Geochemistry of Base Metal Deposits	A. P. Gize
11:20 to 11:50	Discussion	
11:50	Closing Remarks and Discussion	L. M. Cathles
12:30	Lunch—The Nittany Lion Inn	

Friday Afternoon

Faculty will be available for consultation, and tours of the facilities can be arranged for those interested.

References

Bodnar, R.J., 1978, Fluid inclusion study of the porphyry copper prospect at Red Mountain, Arizona: Unpub. M.S. thesis, Univ. Arizona, 70p.

Bodnar, R.J., 1982a, Use of fluid inclusions in mineral exploration I: Fluid inclusion phase relations: in review.

Bodnar, R.J., 1982b, Use of fluid inclusions in mineral exploration II: Porphyry-type deposits: in prep.

Bodnar, R.J. and Beane, R.E., 1980, Temporal and spatial variations in hydrothermal fluid characteristics during vein filling in preore cover overlying deeply buried porphyry copper-type mineralization at Red Mountain, Arizona: Econ. Geol., v.75, p. 876-893.

Burnham, C.W.,1979, Magmas and hydrothermal fluids, in Geochemistry of hydrothermal ore deposits, 2nd ed., H.L. Barnes, ed., John Wiley and Sons, New York, p. 71-136.

Etminan, H., 1977, Le porphyre cupifere de Sar Cheshmeh (Iran): Role des fluides dans les mecanismes d´alteration et de mineralisation: Sciences de la terre, memoire no. 34, March, 1977, 249 pp. (in French).

Haynes, F.H. and Titley, S.R., 1980, The evolution of fracture-related permeability within the Ruby Star granodiorite, Sierrita porphyry copper deposit, Pima County, Arizona: Econ. Geol., v. 75, p.673-683.

Moore, W.J. and Nash, J.T., 1974, Alteration and fluid inclusion studies of the porphyry copper ore body at Bingham, Utah: Econ. Geol., v.69, p.631-645.

Nash, J.T., 1976, Fluid inclusion petrology - data from porphyry copper deposits and applications to exploration: U.S. Geological Survey Prof. Paper 907-D, 16pp.

Nash, J.T. and Cunningham, C.G., 1974, Fluid inclusion studies of the porphyry copper deposit at Bagdad, Arizona: Jour. Research U.S. Geological Survey, v. 2, p. 31-34.

Preece, R.K. and Beane, R.E., 1982, Contrasting evolutions of hydrothermal alteration in quartz monzonite and quartz diorite at the Sierrita porphyry copper deposit, Arizona: Econ. Geol., in press.

Roberts, S.A., 1973, Pervasive early alteration in the Butte district, Montana: Guidebook for the Butte Field Meeting of the Society of Economic Geologists, Aug. 18-21, 1973, p. HH1-HH8.

Roedder, E., 1971, Fluid inclusion studies on the porphyry-type ore deposits at Bingham, Utah, Butte, Montana, and Climax, Colorado: Econ. Geol., v. 66, p. 98-120.

Roedder, E. and Bodnar, R.J., 1980, Geologic pressure determinations from fluid inclusion studies: Ann. Rev. Earth and Planetary Sci., v.8, p.263-301.

Sourirajan,S. and Kennedy, G.C., 1962, The system H_2O-NaCl at elevated temperatures and pressures: Amer. Jour. Sci., v.260, p.115-141.

Figure 1. Isotherms showing the compositions of coexisting phases in the H_2O-NaCl system. Data from Sourirajan and Kennedy, 1962.

Figure 2. Summary of characteristics of fluid inclusions from porphyry copper deposits. L = liquid phase, V = vapor phase, H = halite, X = solid phase other than halite or sylvite. Homogenization temperature (Th) in ^{o}C, salinity in weight percent NaCl equivalent. (From Bodnar, 1982b)

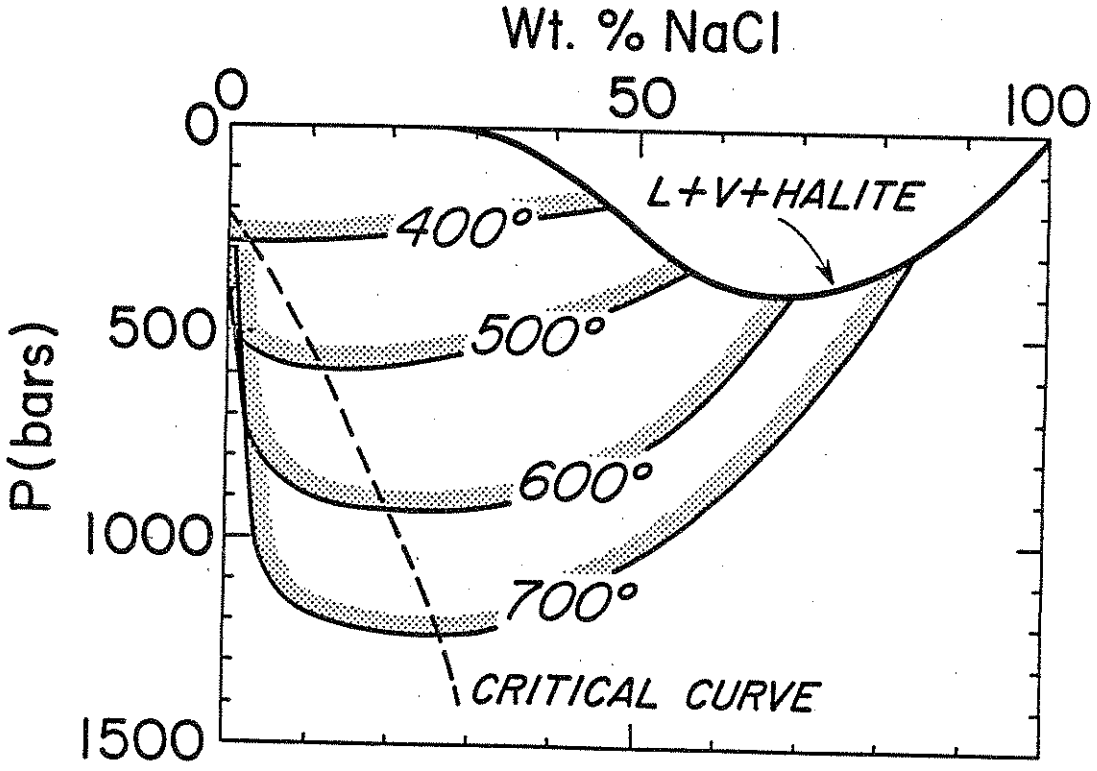

SUMMARY OF PORPHYRY COPPER FLUID INCLUSION DATA

INCLUSION TYPE	Th	SALINITY
L + V ± X ⟶ L	100 — 600	0 — 25
L + V ± X ⟶ V	350 — 700	0 — 25
L+V+H ± X ⟶ L+V ⟶ L	250 — 900	30 — 70
L+V+H ± X ⟶ L+H ⟶ L	150 — 400	30 — 45
L+V+H ± X ⟶ L	150 — 600	30 — 70

Figure 3. Room temperature (25°C) phase relations of H_2O-NaCl fluid inclusions having salinities of 0, 5, 10, 15, 20 and 25 weight percent NaCl and homogenization temperatures from 100°C to the critical point for each composition. Also shown are the room temperature phase relations of inclusions that trapped the vapor phase that would have been in equilibrium with the liquid phase at each temperature. Black corresponds to the vapor phase and the unshaded portion represents the liquid phase. (From Bodnar, 1982a)

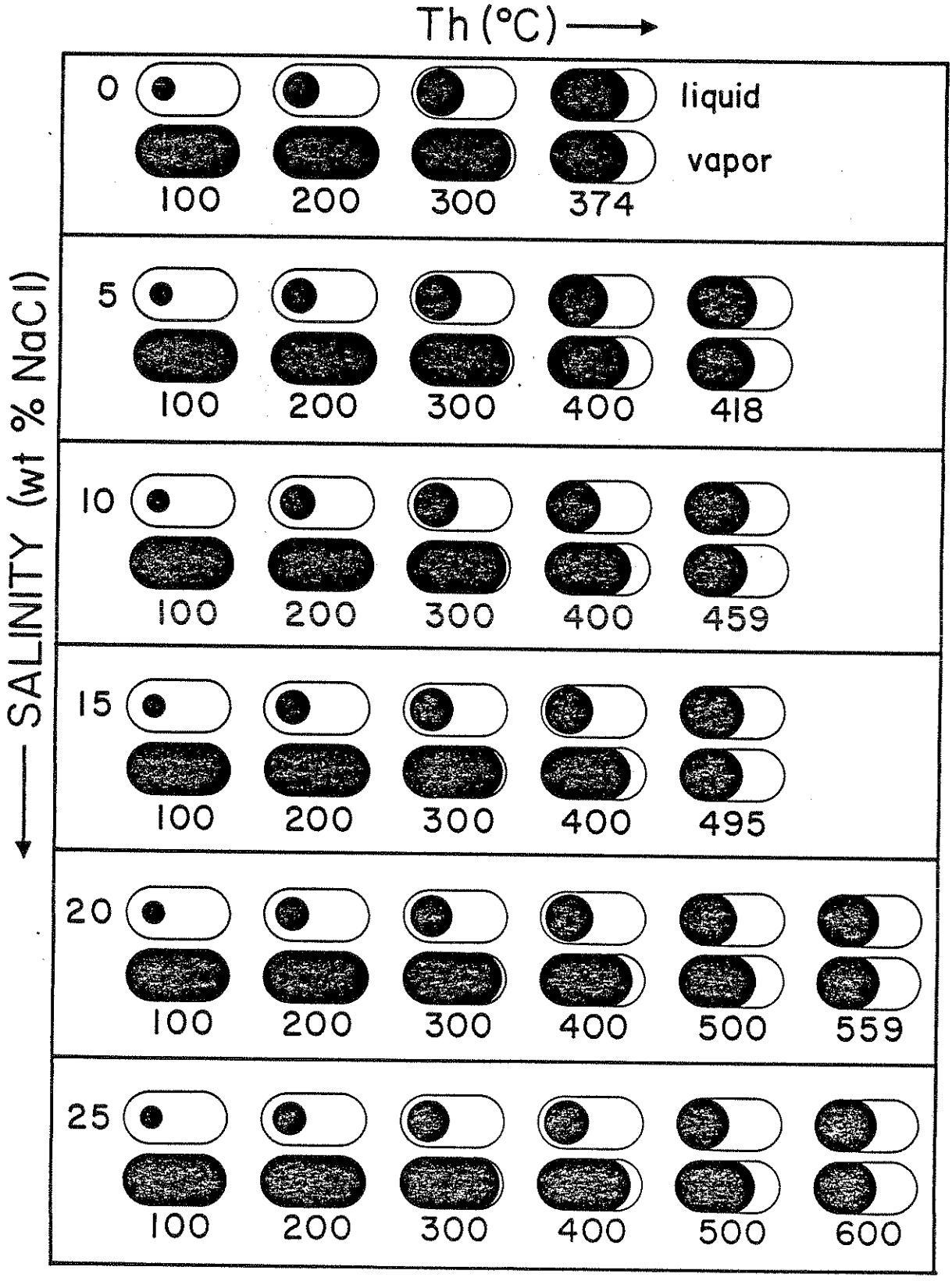
Th (°C) ⟶
SALINITY (wt % NaCl) ⟵
liquid
vapor
0
100
200
300
374
5
100
200
300
400
418
10
100
200
300
400
459
15
100
200
300
400
495
20
100
200
300
400
500
559
25
100
200
300
400
500
600

Figure 4. Room temperature phase relations of H_2O-NaCl fluid inclusions having salinities of 30, 40, 50, 60 and 70 weight percent NaCl and liquid-vapor homogenization temperatures of 100° to 700°C or the critical point, whichever is lower. Also shown are the room temperature phase relations of fluid inclusions that trapped the vapor phase that would have been in equilibrium with the liquid phase at each temperature. Vapor-rich inclusions are not shown with inclusions that homogenize by halite dissolution because these inclusions could not have been trapped in equilibrium with a vapor phase. Black represents vapor, squares or rectangles represent halite and the unshaded portion of each inclusion represents halite-saturated liquid. (From Bodnar, 1982a)

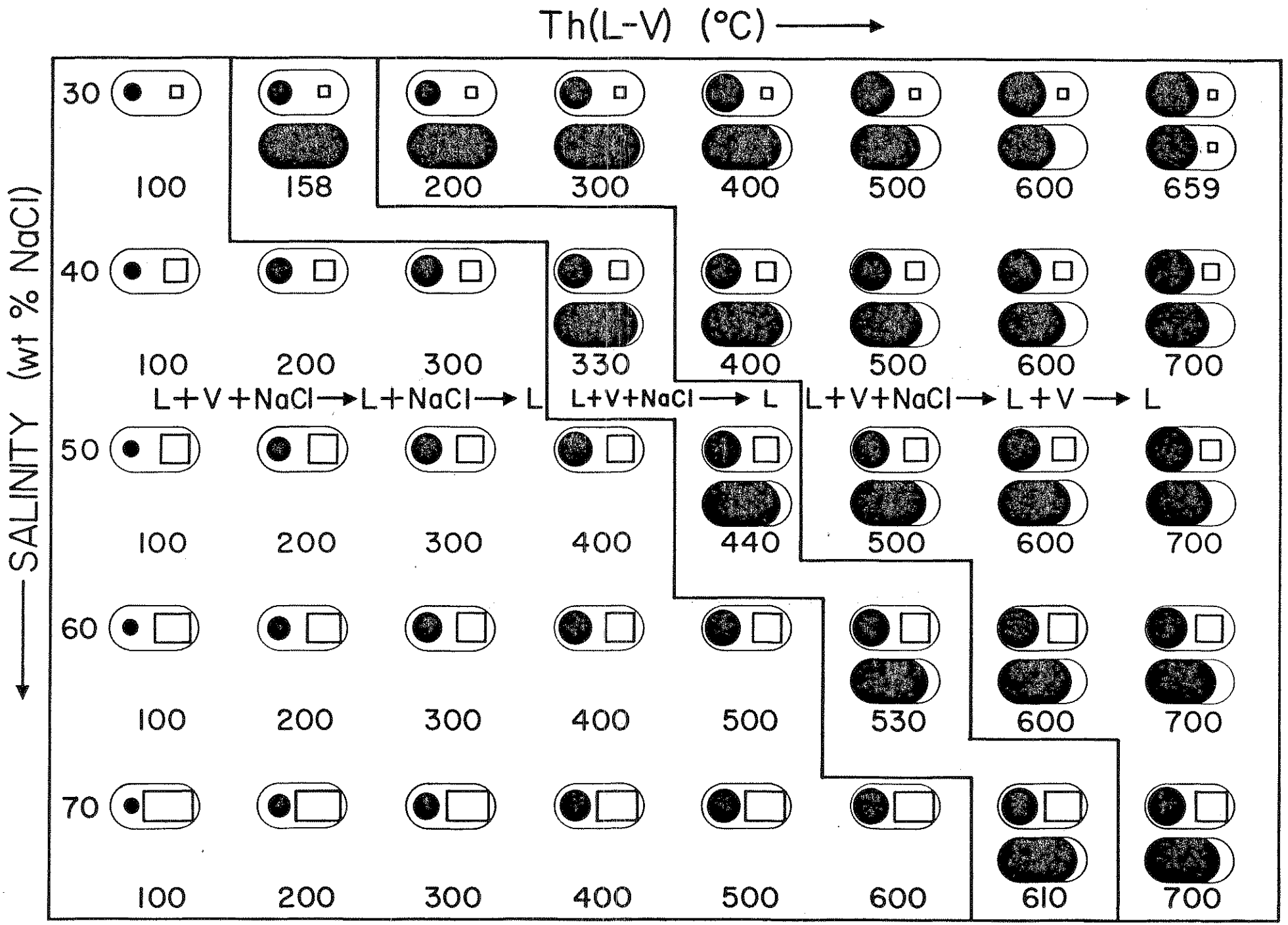
Th(L-V) (°C) ⟶
SALINITY (wt % NaCl) ⟵
30
100
158
200
300
400
500
600
659
40
100
200
300
330
400
500
600
700
L+V+NaCl → L+NaCl → L
L+V+NaCl → L
L+V+NaCl → L+V → L
50
100
200
300
400
440
500
600
700
60
100
200
300
400
500
530
600
700
70
100
200
300
400
500
600
610
700

RB-9

Figure 5. Relationship between the temperature of disappearance of salt (T_{salt}) and the temperature of disappearance of the vapor bubble (T_{L-V}) for halite-bearing inclusions from Red Mountain, Arizona. (From Bodnar, 1978)

Figure 6. P-T diagram showing three different modes of homogenization for halite-bearing inclusions. Inclusion "A" contains 30 weight percent NaCl. When heated this inclusion follows the liquid+vapor+NaCl curve until the halite dissolves at 158°C, and then follows the 30 weight percent liquid+vapor curve until the inclusion homogenizes by bubble disappearance at 400°C. This inclusion could have been trapped at point "A" or any other temperature and pressure along the isochore originating at point "A". Inclusion "B" contains 46 weight percent NaCl. When heated this inclusion follows the liquid+vapor+NaCl curve until both the bubble and the halite disappear at 400°C (point "B"). This inclusion could have been trapped at "B" or at any temperature and pressure along the isochore originating at point "B". Inclusion "C" contains 46 weight percent NaCl. When heated this inclusion follows the liquid+vapor+NaCl curve until the vapor bubble disappears at 310°C. With continued heating the inclusion crosses the liquid+halite field until it intersects the liquidus for 46 weight percent NaCl (point "C"). This inclusion could have been trapped at "C" or at any temperature and pressure along the isochore originating at point "C". (From Roedder and Bodnar, 1980)

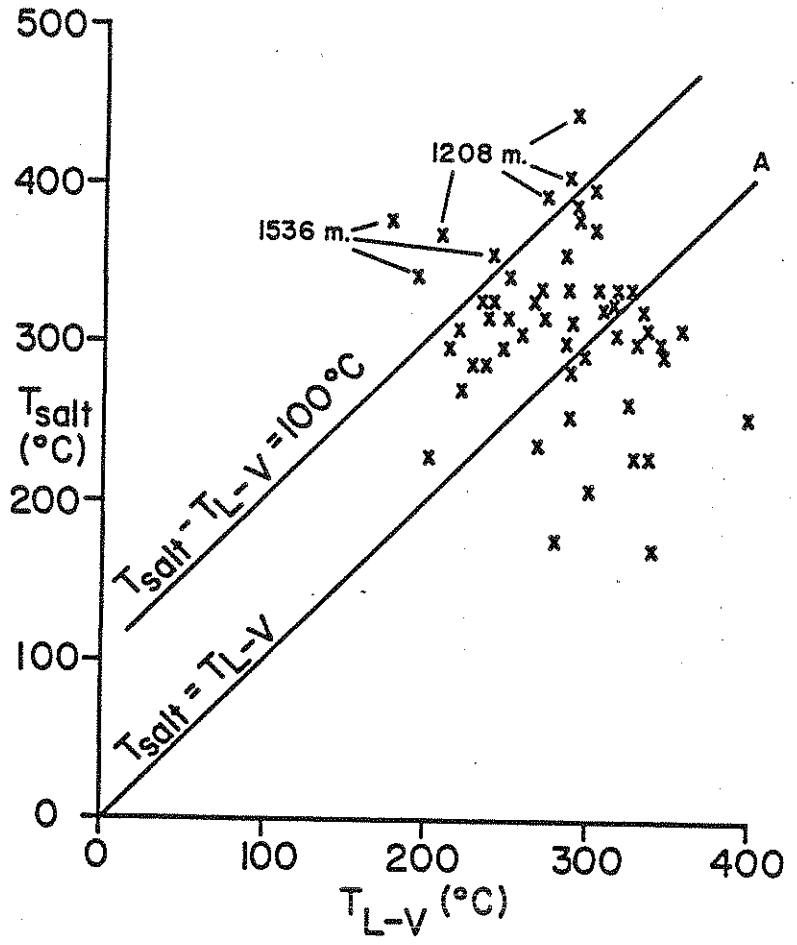
500
400
300
200
100
0
T_{salt} (°C)
1208 m.
1536 m.
A
$T_{salt} - T_{L-V} = 100°C$
$T_{salt} = T_{L-V}$
0
100
200
300
400
T_{L-V} (°C)

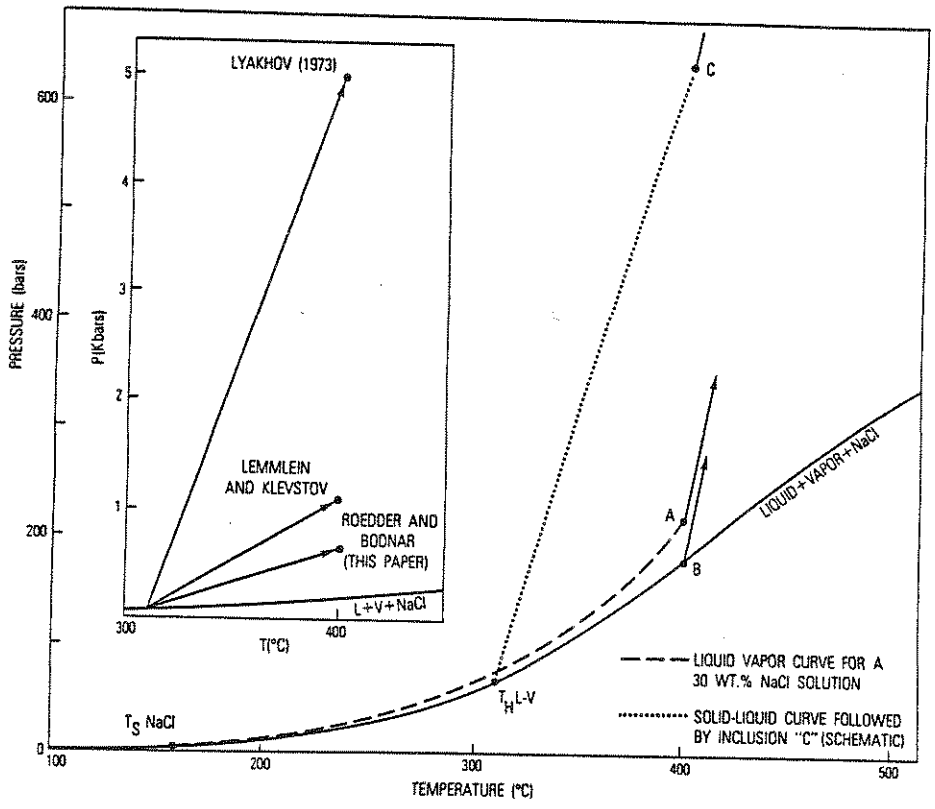
LYAKHOV (1973)
LEMMLEIN AND KLEVSTOV
ROEDDER AND BODNAR (THIS PAPER)
L+V+NaCl
P(Kbars)
T(°C)
PRESSURE (bars)
TEMPERATURE (°C)
C
A
B
LIQUID+VAPOR+NaCl
T_S NaCl
T_H L-V
LIQUID VAPOR CURVE FOR A 30 WT.% NaCl SOLUTION
SOLID-LIQUID CURVE FOLLOWED BY INCLUSION "C" (SCHEMATIC)

Figure 7. Isotherms showing the compositions of coexisting phases in the system H_2O-NaCl. Also shown are P-X projections of the liquidi that intersect the liquid+vapor+solid curve at 158°C (30 weight percent NaCl) and 400°C (45 weight percent NaCl). (From Bodnar, 1982b)

Figure 8. P-T diagram for H_2O-NaCl showing the range of temperatures and pressures over which fluid exsolution from a magma, condensation of the first generation magmatic aqueous fluid phase, and intersection of the liquid+solid field are "permitted" based on fluid inclusion characteristics of porphyry copper deposits. (From Bodnar, 1982b)

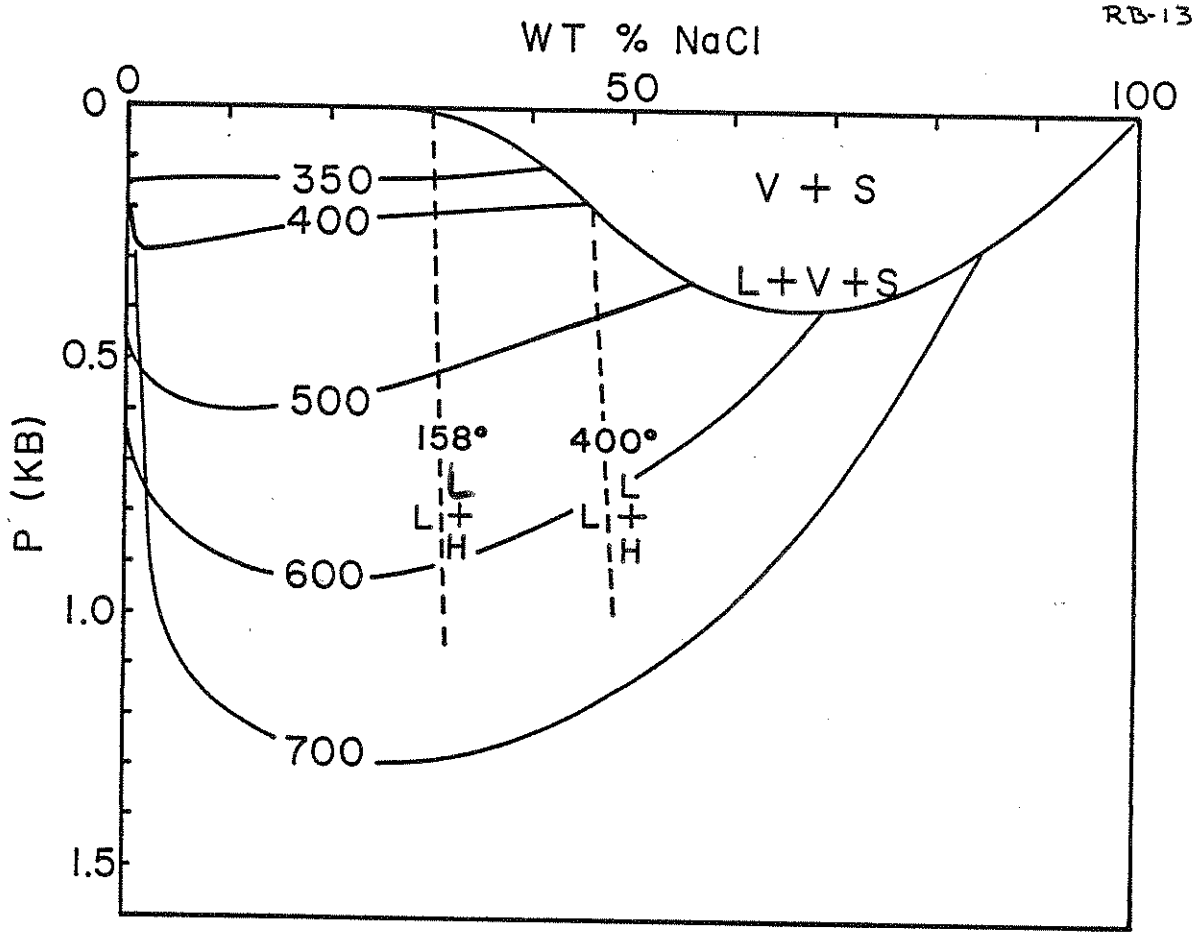
WT % NaCl
0
50
100
0
0.5
1.0
1.5
P (KB)
350
400
500
600
700
V + S
L+V+S
158°
400°
L
L + H

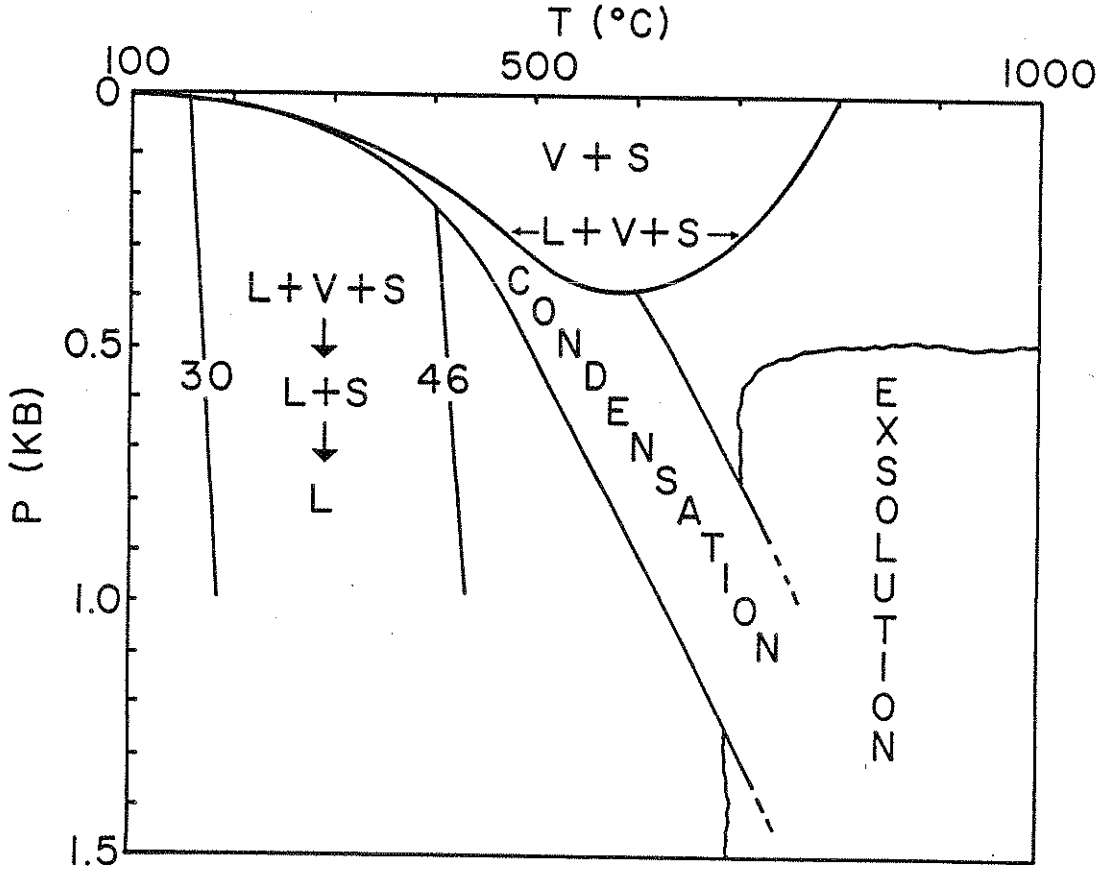
T (°C)
100
500
1000
0
0.5
1.0
1.5
P (KB)
V + S
←L+V+S→
L+V+S
L+S
L
30
46
CONDENSATION
EXSOLUTION

Figure 9. Schematic cross-section of a "typical" porphyry copper intrusion in the early stages of cooling. The unshaded central portion of the diagram represents water-undersaturated magma, surrounded by a water-saturated carapace (circle pattern) and an outer rind of quartz monzonitic-to-granodioritic composition. (Modified from Burnham, 1979)

Figure 10. Flow chart showing the distribution of copper between various rock, melt and aqueous fluid phases during the evolution of a porphyry copper system. The distribution of copper between oceanic basalt and melt is for 20 percent partial melting of the basalt (Burnham, 1979). The partition coefficient (D) of copper between melt and first generation magmatic aqueous phase is from Candela (personal communication, 1981). Copper is distributed between all other aqueous phases proportional to the distribution of chlorine between those same phases as given by Sourirajan and Kennedy (1962).

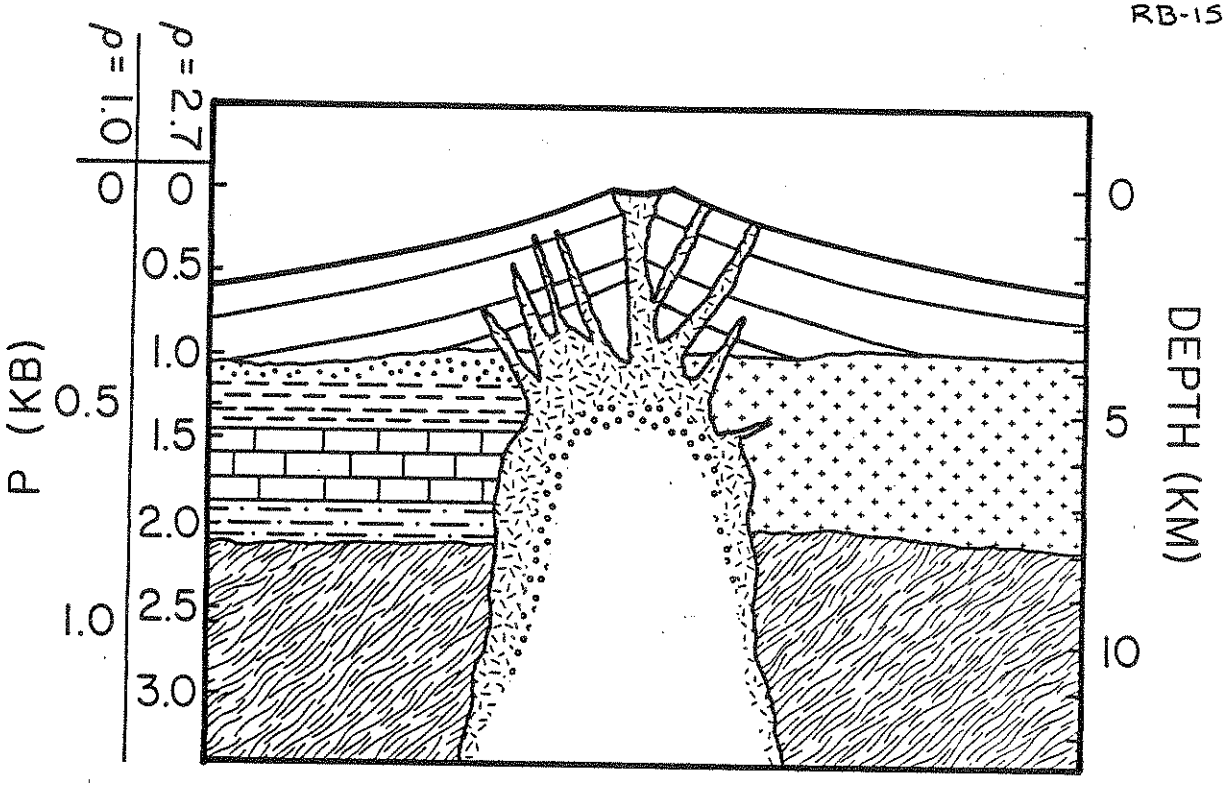

OCEANIC BASALT
80 ppm Cu

partial melting

MELT
400

D =
Cu(aq)/Cu(melt) ≈ 10 X mol. *vapor separation*

1st Generation Magmatic
AQUEOUS PHASE
4000

Cl(liq)/Cl(vapor) ≈ 2.5 *condensation*

2nd Generation Magmatic
AQUEOUS PHASE

LIQUID	VAPOR
18000	1400

Cl(liq)/Cl(vapor) ≈ 50 *condensation*

3rd Generation Magmatic
AQUEOUS PHASE

LIQUID	VAPOR
5000	400

Figure 11. P-X projection of the 600°C isotherm in the H_2O-NaCl system showing the composition, density and mass and volume percents of the coexisting phases at 800 bars. Also shown are the room temperature phase relations of fluid inclusions that trapped either the liquid phase or the vapor phase at 600°C and 800 bars and the room temperature phase relations of an inclusion that trapped a 10 weight percent NaCl fluid at 750°C and 1300 bars. (From Bodnar, 1982b)

Figure 12. P-X projection of a portion of the H_2O-NaCl phase diagram showing the compositions and densities of coexisting liquid and vapor phases at 400°C and 250 bars. Also shown are the mass and volume percents of each of the phases and the 25°C phase relations of fluid inclusions that trapped the liquid or the vapor phase at 400°C, 250 bars. (From Bodnar, 1982b)

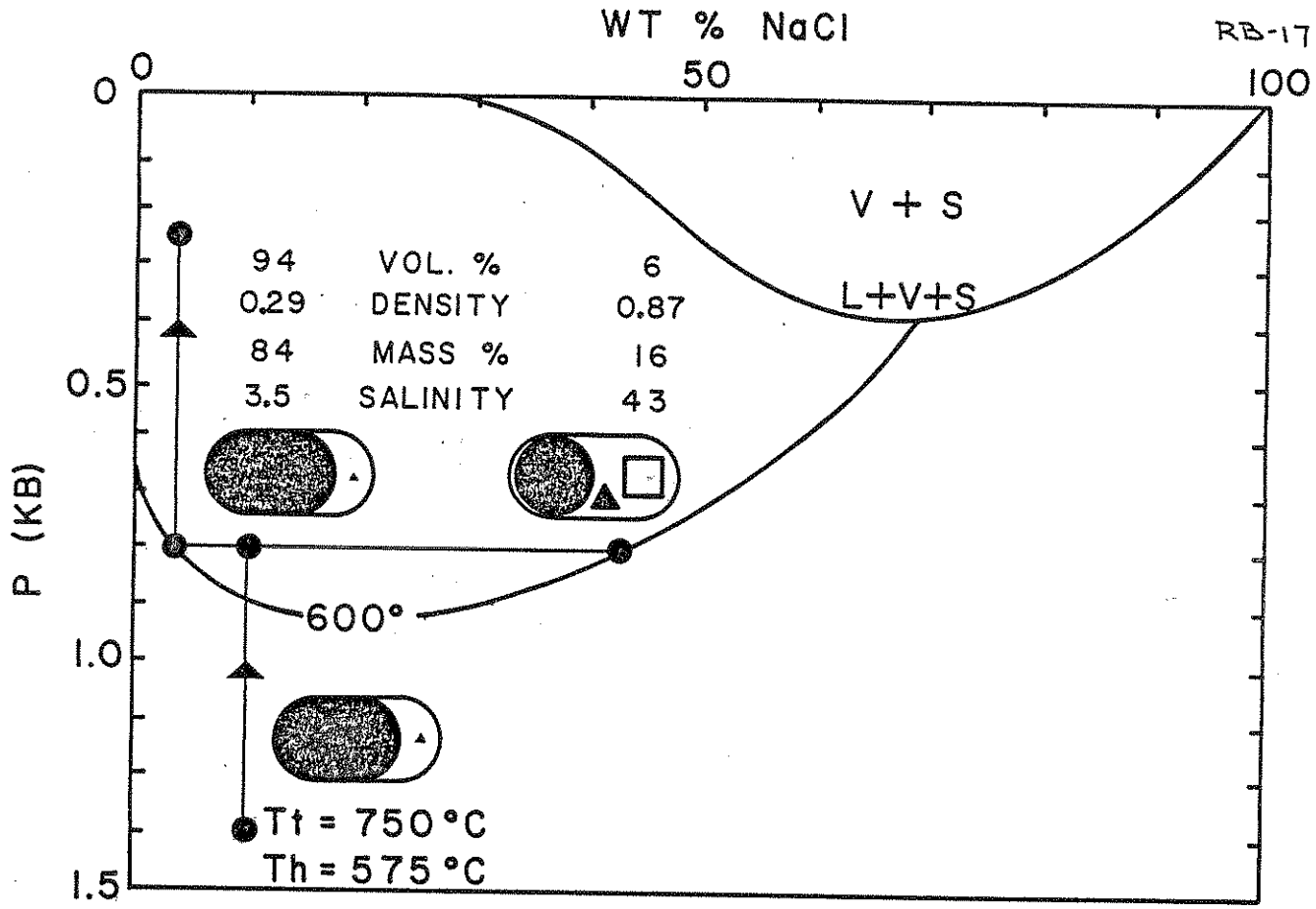
WT % NaCl
RB-17
0
50
100
0
0.5
1.0
1.5
P (KB)
V + S
L+V+S
94
VOL. %
6
0.29
DENSITY
0.87
84
MASS %
16
3.5
SALINITY
43
600°
Tt = 750 °C
Th = 575 °C

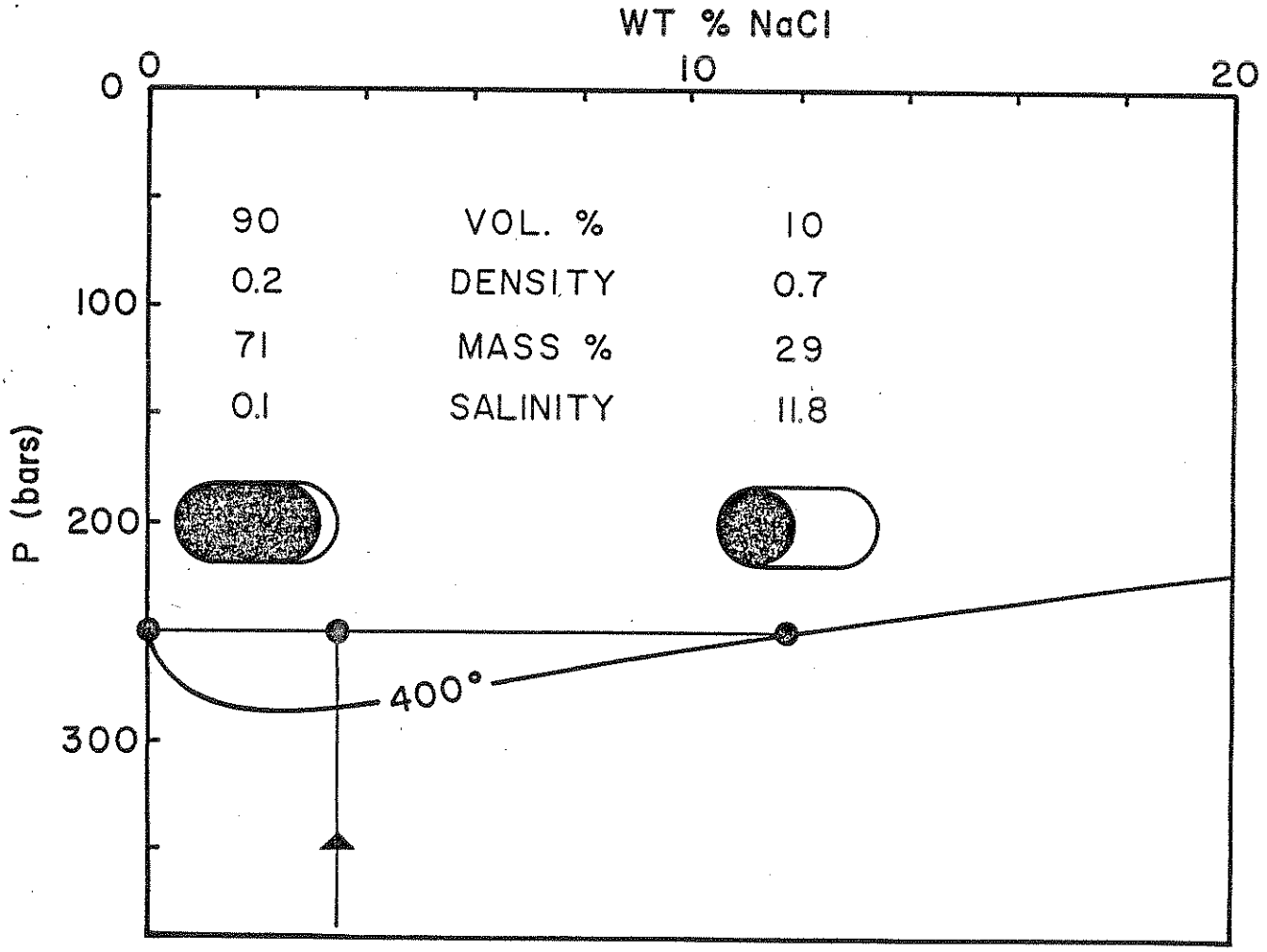
WT % NaCl
0
10
20
100
200
300
P (bars)
90
VOL. %
10
0.2
DENSITY
0.7
71
MASS %
29
0.1
SALINITY
11.8
400°

Figure 13. Variation in relative ages of different fluid inclusion types between the center and periphery of a porphyry copper system at a depth corresponding to the level of exposure of most active deposits in the southwestern U.S., and between deep and shallow portions of the system near the center of the deposit. Relative ages of inclusions are not correlative from one location to another. (From Bodnar, 1982b)

Figure 14. Generalized cross section perpendicular to the c-axis of a milky quartz crystal from Red Mountain, Arizona, (top) and generalized homogenization temperature variations during crystal growth (bottom). Also shown on the bottom portion of this figure are the period of crystal growth in which boiling occurred and the distribution of fluid inclusion types perpendicular to the c-axis. (From Bodnar and Beane, 1980)

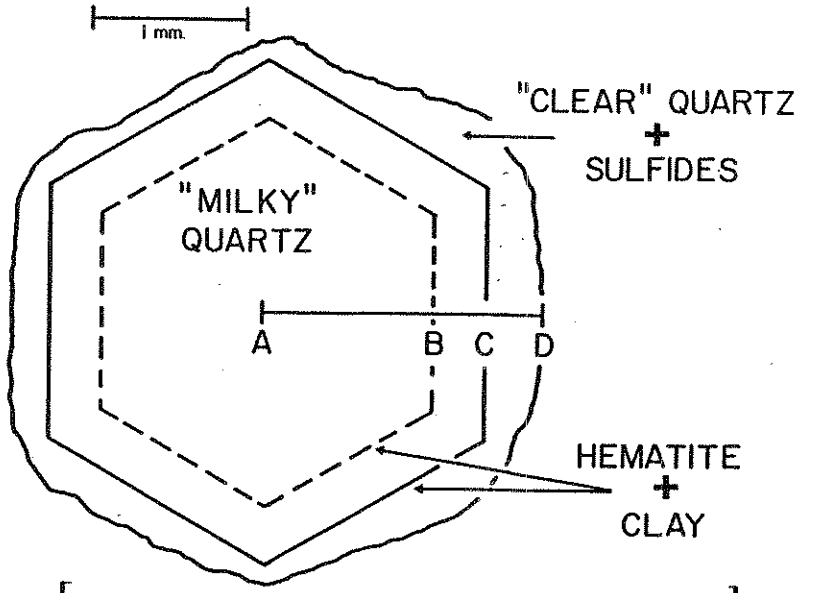
1 mm.
"CLEAR" QUARTZ
+
SULFIDES
"MILKY"
QUARTZ
A
B
C
D
HEMATITE
+
CLAY

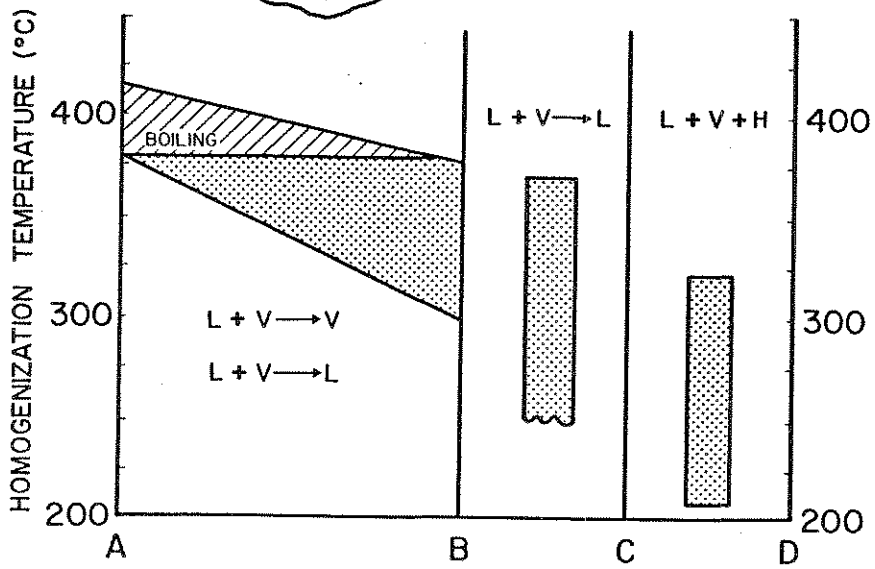
HOMOGENIZATION TEMPERATURE (°C)
400
300
200
BOILING
L + V → V
L + V → L
L + V → L
L + V + H
400
300
200
A
B
C
D

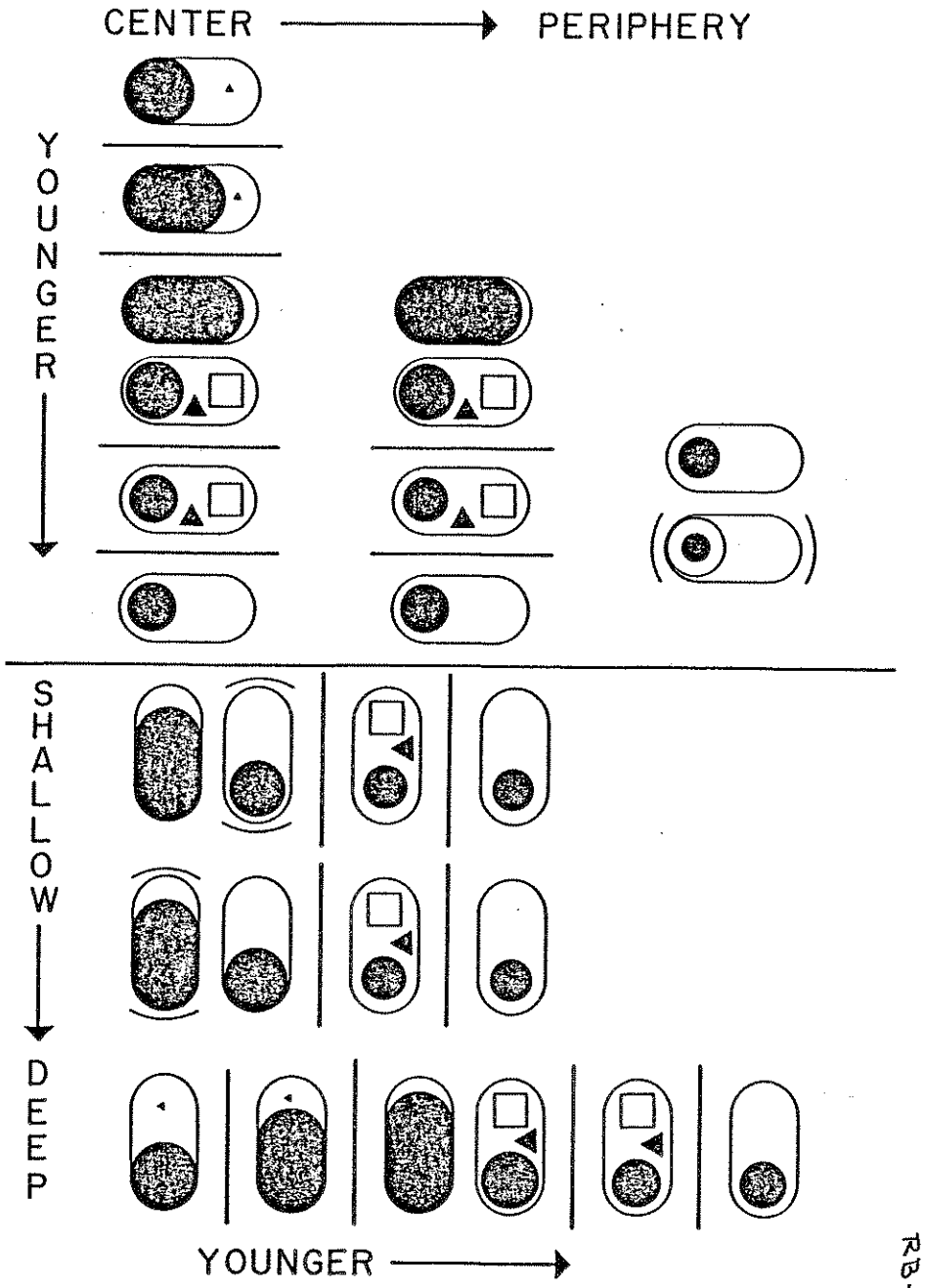
CENTER
PERIPHERY
YOUNGER
SHALLOW
DEEP
YOUNGER

RB-19

Figure 15. P-T projection showing phase boundaries for a 10 weight percent NaCl bulk composition. The right side of this figure shows the room temperature phase relations of fluid inclusions trapped at points 1-4 on the P-T projection. (From Bodnar, 1982b)

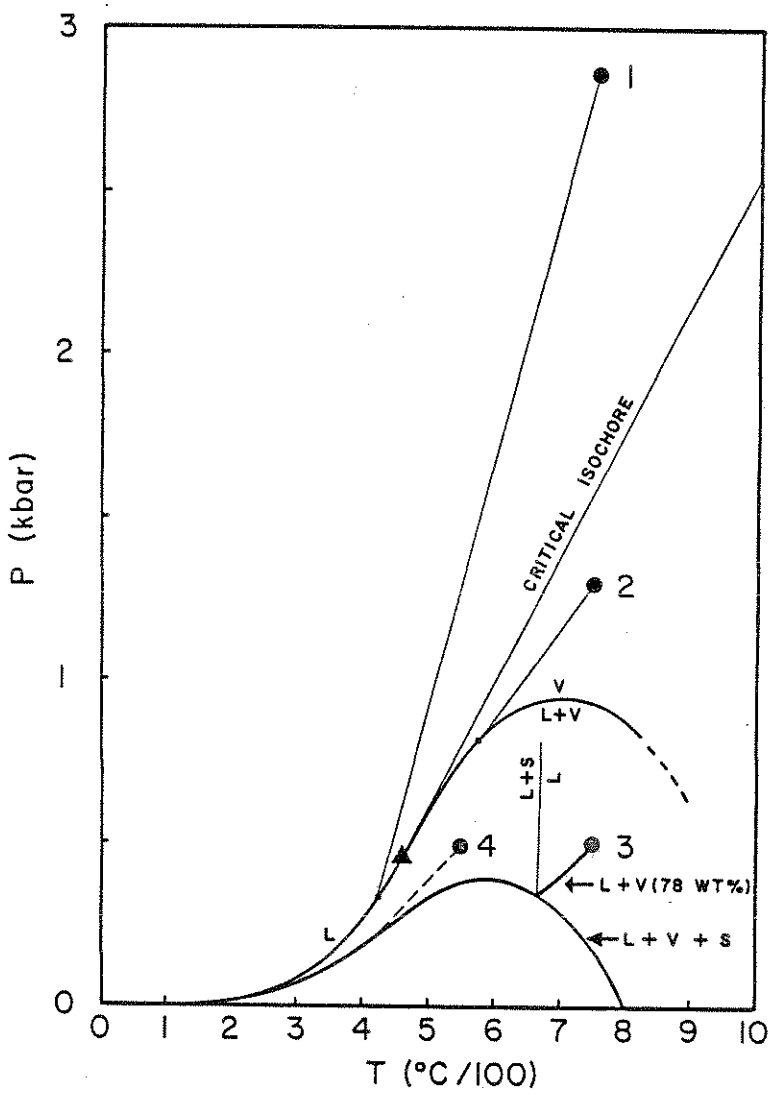

		Tt	Pt	Th
1		750	2.8	430 (L)
2		750	1.3	575 (V)
3		750	0.5	665 (NaCl) 750 (L-V)
		750	0.5	750 (V)
4		550	0.5	~400 (L-V). 550 (NaCl)

Figure 16. Enlargement of the central portion of Figure 15 (400°–750°C, 200–1000 bars) showing the composition of the liquid phase in the liquid+vapor field for a bulk composition of 10 weight percent NaCl. (From Bodnar, 1982b)

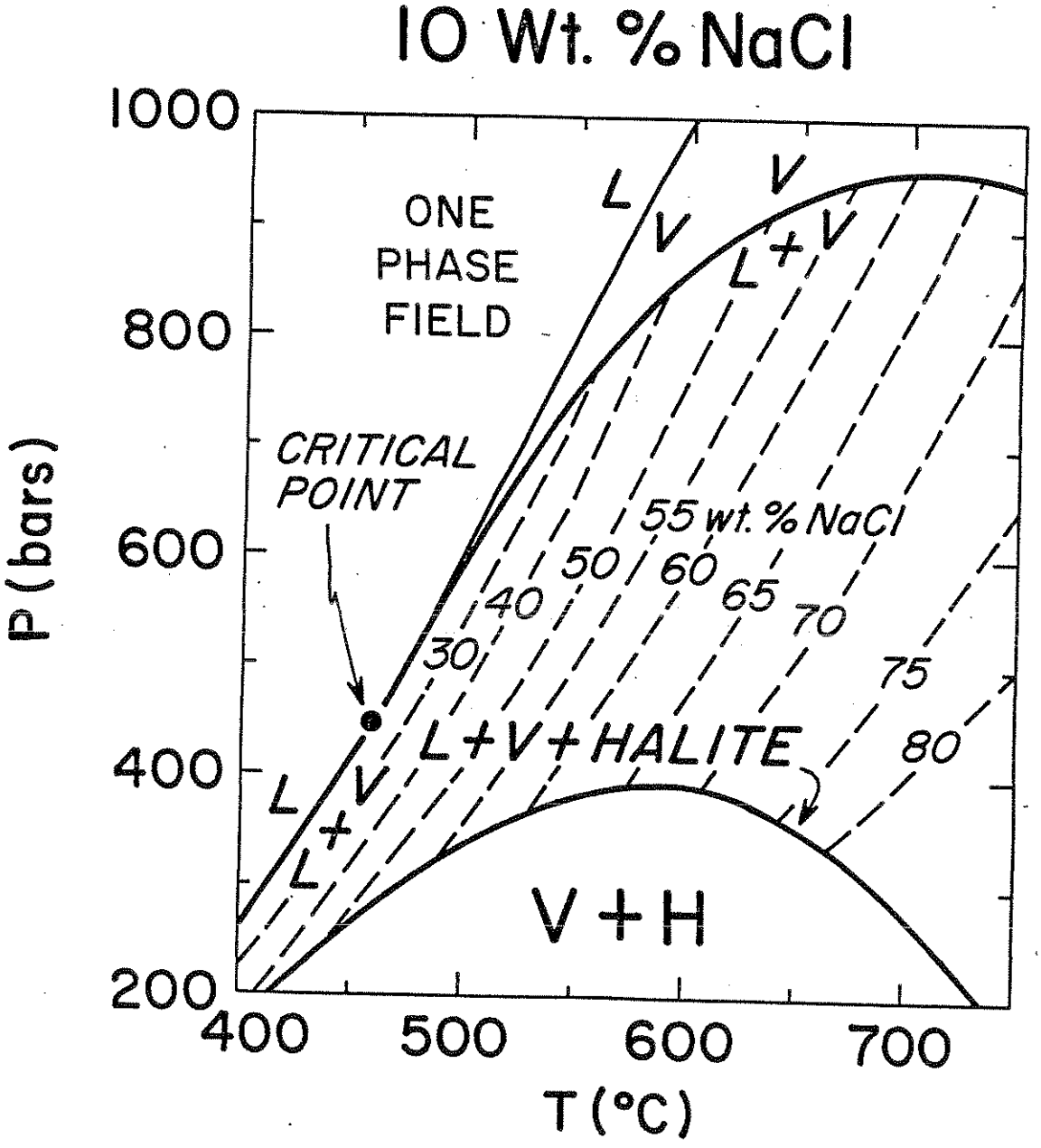
10 Wt. % NaCl
1000
800
600
400
200
P (bars)
400
500
600
700
T (°C)
ONE
PHASE
FIELD
CRITICAL
POINT
L
V
L+V
55 wt. % NaCl
50
60
40
65
70
30
75
80
L+V+HALITE
V+H

Figure 17. Homogenization temperatures of liquid-rich, vapor-rich and halite-bearing inclusions in sample RM11 from Red Mountain, Arizona. The lined pattern on the middle histogram denotes the temperature range in which the histograms for liquid-rich and vapor-rich inclusions overlap (375°-425°C) and corresponds to the temperature range in which boiling occurred. (From Bodnar and Beane, 1980)

Figure 18. Method of quantifying characteristics and distribution of fluid inclusions in porphyry copper deposits to establish a numerical index for use in exploration. The maximum value assigned to each characteristic is proportional to the suggested importance of that characteristic. Values of the index range from 0-22 with higher values indicating a higher probability of porphyry copper mineralization. (From Bodnar, 1982b)

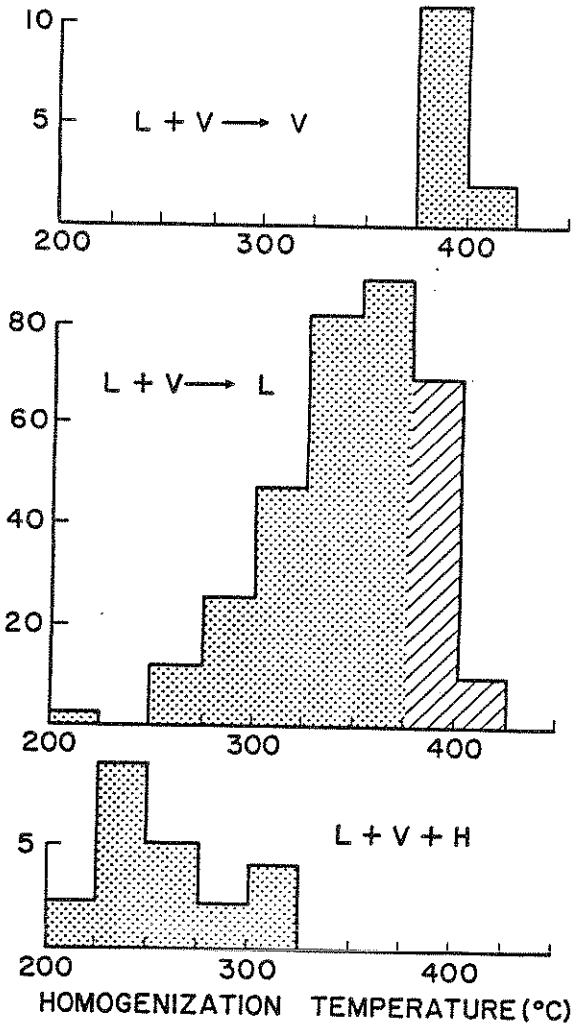

CHARACTERISTIC	REL. ABUNDANCE
HALITE—BEARING INCLUSIONS	0 → 12
VAPOR—RICH INCLUSIONS	0 → 6
CHALCOPYRITE DAUGHTER MINERALS	0 → 4

PORPHYRY CU PROBABILITY INDEX = Σ